High T_g, Nonpoled Photorefractive Polymers

Huawei Li,[†] Roberto Termine,[†] Luigi Angiolini,[‡] Loris Giorgini,[‡] Francesco Mauriello,[‡] and Attilio Golemme[†,*]

Centro di Eccellenza CEMIF.CAL, LASCAMM CR-INSTM, Licryl CNR-INFM, Dipartimento di Chimica, Università della Calabria, 87036 Rende, Italy, and Dipartimento di Chimica Industriale e dei Materiali and INSTM UdR-Bologna, University of Bologna, Viale Risorgimento 4, 40136 Bologna, Italy

Received December 23, 2008. Revised Manuscript Received April 16, 2009

Room-temperature photorefractivity without prepoling was demonstrated in polymers and copolymers with a glass transition temperature well above 100 °C. The compounds used are multifunctional side-chain polymers exhibiting chiral, semiconducting, photochromic, and nonlinear optical (azoaromatic moieties) properties. The photorefractive performance was linked to the reorientational effect of the photogenerated space-charge field, which well below the glass transition temperature can be active in the presence of the conformational mobility achieved via the trans−cis light-induced isomerization. The grating build-up time, which is long at $\lambda = 633$ nm (with a time constant $\tau \approx 500-1000$ s) decreases by 2 orders of magnitude at $\lambda = 532$ nm, where absorption is higher.

Introduction

In recent years, the development of organic materials for optoelectronics and photonics has been continuously progressing, driven by the prospect of manufacturing flexible, low-cost devices with tailorable properties for specific applications. Among the different functionalities investigated, the photorefractive (PR) one is relevant for a variety of applications, ranging from holography[1,2] to image processing.[3,4] Photorefractive materials are photoconductors in which the space redistribution of charges photogenerated by a nonuniform illumination creates an electric field. In turn, such space-charge field affects the refractive index if the material exhibits nonlinear optical properties and/or spontaneous (or field-induced) birefringence. The resulting hologram is then phase-shifted with respect to the illumination pattern,[5,6] a property unique to PR gratings and with important consequences for applications.

Both low-molecular-weight[7−10] and polymeric[11−13] amorphous organic systems have been extensively studied as PR materials in the last two decades.[14] They may be divided in two general classes, depending on their glass transition temperature (T_g) being above or below the operational temperature, usually room temperature (RT). In the second case, electric-field-induced molecular reorientations are possible during the encoding process, leading to a spatially modulated birefringence and to high refractive index contrast with two (electro-optic and birefringence) contributions.[15] In early systems, the main disadvantage of the low T_g materials was their instability because of phase separation.[16] This problem is not present in monolithic systems, which, however, require more complex synthetic efforts. When T_g is instead higher than RT, in order to obtain macroscopic second-order nonlinear properties, orientational order is induced during the so-called prepoling process, which is needed in order to break the centrosymmetry of the bulk material. The prepoling is an electric field-induced chromophore orientation obtained at temperatures above T_g, followed by a cooling to RT with the field still on. As no birefringence contribution is present, high T_g polymers usually exhibit lower refractive index modulations.

* Corresponding author. E-mail: a.golemme@unical.it. Phone: +39 0984492016. Fax: +39 0984 492138.
† Università della Calabria.
‡ University of Bologna.

(1) Maldonado, J. L.; Ramos-Ortìz, G.; Barbosa-Garcìa, O.; Menenes-Nava, M. A.; Màrquez, L.; Olmos-Lòpez, M. *Int. J. Mod. Phys. B* **2007**, *21*, 2625.
(2) Tay, S.; Blanche, P. A.; Voorakaranam, R.; Tunc, A. V.; Lin, W.; Rokutanda, S.; Gu, T.; Flores, D.; Wang, P.; Li, G.; St Hilaire, P.; Thomas, J.; Norwood, R. A.; Yamamoto, M.; Peyghambarian, N. *Nature* **2008**, *451*, 694.
(3) Grunnet-Jepsen, A.; Thompson, C. L.; Moerner, W. E. *Science* **1997**, *277*, 549.
(4) Mecher, E.; Gallego-Gomez, F.; Tillmann, H.; Horhold, H. H.; Hummelen, J. C.; Meerholz, K. *Nature* **2002**, *418*, 959.
(5) Yeh P. *Introduction to Photorefractive Nonlinear Optics*; John Wiley & Sons: New York, 1993.
(6) Solymar, L.; Webb, D. J.; Grunnet-Jepsen A. *The Physics and Applications of Photorefractive Materials*; Oxford University Press: Oxford, U.K., 1996.
(7) Lundquist, P. M.; Wortmann, R.; Geletneky, C.; Twieg, R. J.; Jurich, M.; Lee, V. Y.; Moylan, C. R.; Burland, D. M. *Science* **1996**, *274*, 1182.
(8) Ostroverkhova, O.; Gubler, U.; Wright, D.; Moerner, W. E.; He, M.; Twieg, R. J. *Adv. Funct. Mater.* **2002**, *12*, 621.
(9) He, M.; Twieg, R. J.; Gubler, U.; Wright, D.; Moerner, W. E. *Chem. Mater.* **2003**, *15*, 1156.
(10) Zhang, L.; Shi, J.; Jiang, Z. W.; Huang, M.; Chen, Z.; Gong, Q.; Cao, S. *Adv. Funct. Mater.* **2008**, *18*, 362.
(11) Ducharme, S.; Scott, J. C.; Twieg, R. J.; Moerner, W. E. *Phys. Rev. Lett.* **1991**, *66*, 1846.
(12) Meerholz, K.; Volodin, B. L.; Sandalphon, Kippelen, B.; Peyghambarian, N. *Nature* **1994**, *371*, 497.
(13) Kwon, O. P.; Lee, S. H.; Montemezzani, G.; Günter, P. *Adv. Funct. Mater.* **2003**, *13*, 434.
(14) Ostroverkhova, O.; Moerner, W. E. *Chem. Rev.* **2004**, *104*, 3267.
(15) Moerner, W. E.; Silence, S. M.; Hache, F.; Bjorklund, G. C. *J. Opt. Soc. Am., B* **1994**, *11*, 320.
(16) Kippelen, B.; Marder, S.; Hendrickx, E.; Maldonado, J. L.; Guillemet, G.; Volodin, B. L.; Steele, D. D.; Enami, Y.; Sandalphon; Yao, Y. L.; Wang, J. F.; Rockel, H.; Erskine, L.; Peyghambarian, N. *Science* **1998**, *279*, 54.

10.1021/cm8034664 CCC: $40.75 © 2009 American Chemical Society
Published on Web 05/01/2009

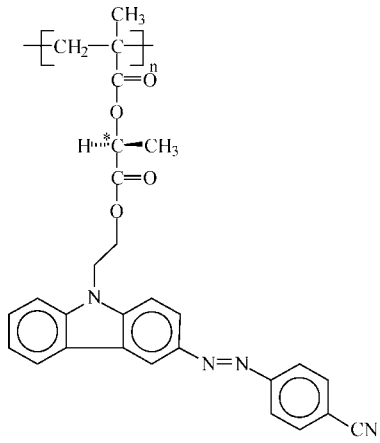

1 Poly[(*S*)-**MLECA**]

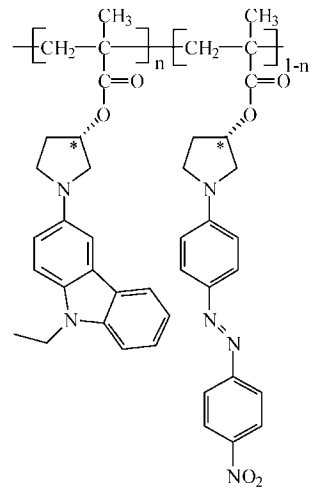

2 Poly[(*S*)-(−)-**MECP**-*co*-(*S*)-**MAP-N**] (50/50) n=0.50

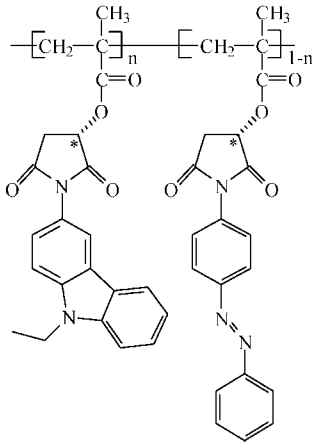

3 Poly[(*S*)-(+)-**MECSI**-*co*-(*S*)-(+)-**MOSI**] (24/76) n=0.24
4 Poly[(*S*)-(+)-**MECSI**-*co*-(*S*)-(+)-**MOSI**] (76/24) n=0.76

Figure 1. Molecular structures of the investigated homopolymer and copolymers.

Table 1. Relevant Characterization Data of the Investigated Polymeric Derivatives

compd	$\bar{M}_n$[a] (g mol^{-1})	$\bar{M}_w/\bar{M}_n$[a]	α^b (cm^{-1})	$T_g{}^c$ (°C)	$T_d{}^d$ (°C)	σ_{ph}/I^e (Ω^{-1} cm W^{-1})
1			1811			
poly[(*S*)-**MLECA**]	13400	1.8	168	147	363	6.15×10^{-14}
2						
poly[(*S*)-(−)-**MECP**-*co*-(*S*)-**MAP-N**] 50/50	6700	1.5	(692)	(107)	328	(2.12×10^{-10})
3			358			
poly[(*S*)-(+)-**MECSI**-*co*-(*S*)-(+)-**MOSI**] 24/76	9400	1.9	68	227	297	$<1 \times 10^{-15}$
4			527			
poly[(*S*)-(+)-**MECSI**-*co*-(*S*)-(+)-**MOSI**] 76/24	10200	2.0	75	228	298	4.10×10^{-13}

[a] Determined by SEC in THF solution at 25 °C. [b] Measured on solid films at $\lambda = 532$ nm (above) and $\lambda = 633$ nm (below). Between brackets are the values for the mixtures containing 20% of the DDP plasticizer. [c] Glass-transition temperature of pure compounds determined by DSC at 10 °C/min heating rate under nitrogen flow (between brackets the values for the mixtures containing 20% of the DDP plasticizer). [d] Initial decomposition temperature as determined by TGA at 20 °C/min heating rate under air flow. [e] Photoconductivity normalized with respect to the light intensity $I = 0.8$ W/cm^2, measured at an applied field $E = 30$ V/μm, using light with a wavelength $\lambda = 633$ nm (between brackets the values for the mixtures containing 20% of the DDP plasticizer).

Field-induced reorientations at the molecular level are then of particular relevance in PR organic materials. In the following, we will show how, even at temperatures well below T_g, molecular reorientations can be induced in polymers in order to obtain a PR response. This feature is particularly interesting, because it allows for the elimination of the poling step while at the same time adding a birefringence contribution to the index modulation. In other words, it will be shown how high T_g organics can have a PR behavior similar to the one exhibited by their low T_g counterpart when molecular mobility is induced by some externally applied stimulus, such as the writing illumination itself.

Experimental Section

Polymers. Structures, molecular weight distributions, and thermal characterisations of the studied polymers, obtained by AIBN initiated radical polymerization, are shown in Figure 1 and Table 1. Poly[(*S*)-(4-cyanophenyl)-[3-[9-[2-(2-methacryloyloxypropanoyloxy) ethyl]carbazolyl]]diazene] {poly[(*S*)-MLECA]} (**1**) was

synthesized as previously described.[17] The monomers (*S*)-(−)-3-methacryloyloxy-*N*-[3-(9-ethylcarbazolyl)]pyrrolidine [(*S*)-(−)-MECP] and (*S*)-3-methacryloyloxy-1-(4′-nitro-4-azobenzene)pyrrolidine [(*S*)-MAP-N] were synthesized as described.[18,19] The novel copolymer Poly[(*S*)-(−)-3-methacryloyloxy-*N*-[3-(9-ethylcarbazolyl)]pyrrolidine-*co*-(*S*)-3-methacryloyloxy-1-(4′-nitro-4-azobenzene)pyrrolidine] 50/50 {poly[(*S*)-(−)-MECP-co-(*S*)-MAP-N] 50/50} (**2**) was synthesized and characterized as described in the Supporting Information. Copolymers poly[(*S*)-(+)-2-methacryloyloxy-*N*-[3-(9-ethylcarbazolyl)]succinimide-*co*-(*S*)-(+)-2-methacryloyloxy-*N*-(4-azobenzene)succinimide] 24/76 {poly[(*S*)-(+)-MECSI-co-(*S*)-(+)-MOSI] 24/76} (**3**) and poly[(*S*)-(+)-2-methacryloyloxy-N-[3-(9-ethylcarbazolyl)]succinimide-*co*-(*S*)-(+)-2-methacryloyloxy-N-(4-azobenzene)succinimide] 76/24 {poly[(*S*)-(+)-MECSI-co-(*S*)-(+)-MOSI] 76/24} (**4**) have been synthesized as previously described.[20]

Sample Preparation. Samples were prepared by squeezing substances between two conductive (ITO) hot glasses, controlling the thickness with glass spacers. Cells were then cooled quickly to room temperature and the real thickness was measured by interferometry. Samples containing a plasticizer were prepared by first dissolving the components in chloroform and then, after solvent evaporation, processing the resulting blend according to the method described above. Glass transition temperatures (T_g) were determined using a Pyris DSC (Perkin-Elmer) at a 10 °C min^{-1} heating rate, under a nitrogen flow.

Photoconductivity. Photoconductivity was measured by applying a 30 V μm^{-1} DC electric field and subtracting the dark current from the current measured with the illumination provided by a He−Ne laser. The current was measured using a Kethley 6517A electrometer at a light intensity $I \approx 0.8$ W cm^{-2}. As the current depends on light intensity, photoconductivity data were normalized with respect to *I*.

Optical Characterization. For birefringence detection, samples were illuminated by a weak polarized probe beam ($I \approx 4 \times 10^{-4}$ W/cm^2) propagating at 45° with respect to the sample normal, with a polarization set at 45° with respect to the p-plane (the plane containing the sample normal and the beam). Beyond the sample, the probe beam crossed first a Soleil-Babinet compensator and then a second polarizer (crossed with respect to the probe beam initial polarization) before finally reaching a photodiode detector. The intensity of the probe beam was low enough to avoid the formation of any measurable birefringence. If a birefringence is present, the sample acts as retardation plate, rotating the polarization plane. The intensity of the light reaching the photodiode will then vary according to the following

$$I = I_{max} \sin^2 \frac{\pi d \Delta n}{\lambda \cos \xi_{int}} \quad (1)$$

where *d* is the thickness of the sample, λ is the wavelength of the light, ξ_{int} is the angle between the sample normal and the light direction inside the material, *I* is the measured light intensity, and I_{max} is the maximum light intensity passing through the system, measured by changing the phase retardation of the compensator. Light-induced birefringence was measured by illuminating the sample with a light beam propagating along the sample normal and polarized in a plane normal to the p-plane. During these measurements, a second detector was placed beyond the sample in order to measure the time dependence of the writing beam transmission. Field-induced birefringence was instead measured with just the weak probe beam turned on and by applying an electric field $E = 20$ V/μm along the sample normal.

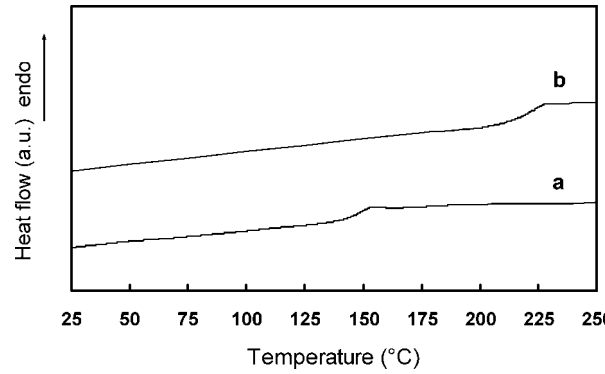

Figure 2. DSC thermograms of compounds (a) **1** and (b) **4**.

Photorefractive Characterization. Two-Beam coupling experiments (2BC) were performed by overlapping on the sample two coherent, p-polarized laser beams with the same intensity (~0.8 W cm^{-2}) and diameter (~0.8 mm). Two different laser sources were used: a He−Ne laser at $\lambda = 633$ nm and a DPSS laser at $\lambda = 532$ nm. The angle between the sample normal and the beams bisector was $\phi = 60°$, and the angle between the beams was $\theta \approx 20°$, corresponding to an interference period $\Lambda \approx 3$ μm. The electrodes of a power supply were connected to the sample in order to apply an electric field. The beams intensities after the sample were monitored by photodiodes and acquired by a chopper/lock-in system. Phase shift measurements were performed using the same setup as for 2BC. Samples were first exposed to the interference pattern for a time long enough to write the grating and then they were translated at a constant rate along the grating wavevector (normal to the fringes) direction. The phase shift value was extracted from the variation of the beams intensities during the translation. To avoid the overwriting of different gratings, the total translation time was kept much lower than the grating formation time.

Results and Discussion

Materials. The chemical structures of the materials used in this study are shown in Figure 1, whereas their T_g values and decomposition temperatures (T_d) are listed in Table 1. Some representative DSC curves are shown in Figure 2 while TGA curves for the same compounds are included within the Supporting Information (Figure S1). Materials were chosen in order to study the PR properties in high T_g multifunctional media exhibiting chiral, semiconducting (carbazole moiety), photochromic, and nonlinear optical (azoaromatic moieties) properties. Chirality is important when such materials are used as chirooptical switches, but it is not a relevant property in the context of this work, and neither is photochromism in itself, although the photoisomerization associated with photochromism is important, as it will be shown in the remainder of this work. Homopolymeric compound **1** bears three distinct functional groups (i.e., the azoaromatic, carbazole, and chiral groups of one single configuration) directly linked to a single side chain. Copolymeric compounds **2**−**4** have two different side-chains: one comonomer with either a (*S*)-3-hydroxy pyrrolidinyl (2) or

(17) Angiolini, L.; Benelli, T.; Giorgini, L.; Mauriello, F.; Salatelli, E. *Macromol. Chem. Phys.* **2006**, *207*, 1805.
(18) Angiolini, L.; Benelli, T.; Giorgini, L.; Golemme, A.; Mauriello, F.; Salatelli, E.; Termine, R. *Macromol. Chem. Phys.* **2008**, *209*, 944.
(19) Angiolini, L.; Caretti, D.; Giorgini, L.; Salatelli, E. *J. Polym. Sci., Part A: Polym. Chem.* **1999**, *37*, 3257.
(20) Angiolini, L.; Benelli, T.; Giorgini, L.; Mauriello, F.; Salatelli, E. *Proc. SPIE* **2007**, 66531, C/1.

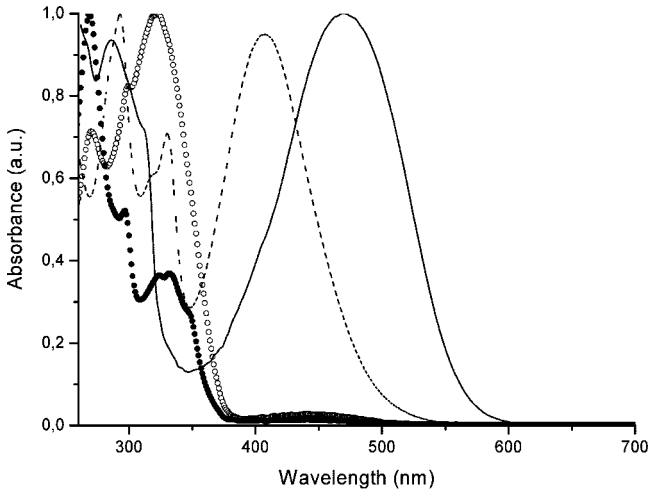

Figure 3. Normalized UV−vis absorption spectra in $CHCl_3$ of **1** (----), **2** (—), **3** (○○○), and **4** (•••).

a (*S*)-2-hydroxy succinimide (**3**,**4**) ring as a chiral moiety, covalently linked to a photochromic azoaromatic group, substituted (**2**) or not (**3**,**4**) in the 4′-position with a nitro (electron withdrawing) residue. In the side-chain of the second kind of comonomer, the same chiral rings are linked to photoconductive carbazolic chromophores. In **2**−**4**, the conformationally rigid pyrrolidine or succinimide rings increase the stiffness of the macromolecules and induce high T_g values (see Table 1). As can be seen from Figure 2, glass transitions are relatively broad (15−20 °C), but all experiments were carried out at least 80 °C (and in most cases much more) below T_g. Strongly electron-withdrawing cyano or nitro groups are present in **1** and **2**, respectively, inducing considerable permanent dipole moments. The normalized UV−vis spectra in diluted solutions ($CHCl_3$) of the investigated polymeric compounds are shown in Figure 3.

Optical Properties. It is well-known that a trans−cis isomerization around the N═N double bond is induced in azo-compounds upon light illumination in the spectral region corresponding to the absorption of the azo-moiety.[21] The thermally activated conversion to a trans configuration of the less-stable cis isomer is usually slower than the light-induced trans to cis isomerization. As a consequence, since the absorption of the two isomers is different, absorption changes because of irradiation. In addition, if linearly polarized light is used, birefringence and linear dichroism can be induced, because molecular orientations with transition dipole moments along the polarization direction are depleted as a consequence of the photoisomerization process.[22−25] Under illumination with an interference pattern, both phase and absorption gratings would then develop within an azo-compound. We defer the presentation of the data on such gratings to the section on photorefractive properties and discuss here light-induced birefringence.

Measurements were conducted as described in the experimental section. Neglecting surface effects, illumination with linearly polarized light is expected to induce a uniaxial anisotropy in the refractive index, with the symmetry axis along the polarization direction. The chosen geometry and polarization are then such that light transmission of the probe beam is sensitive to the full induced birefringence (Δn). Figure 4a shows the birefringence, calculated using eq 1, as a function of illumination time at $\lambda = 633$ nm ($I = 0.4$ W/cm^2) in the case of compound **1**. Similar values of birefringence were obtained for **2**. For **3** and **4**, because of the lower absorption, light-induced birefringence was hardly detectable at $\lambda = 633$ nm but it became again of the order of $\Delta n \approx 1 \times 10^{-3}$ illuminating at $\lambda = 532$ nm, where absorption is higher (see Table 1). As expected, birefringent samples are also dichroic, with absorption coefficients increasing by 20−80 cm^{-1} when the polarization is rotated by $\pi/2$ with respect to the polarization of the light that induced the birefringence. As a general trend, the time constants of birefringence build-up becomes shorter, and birefringence becomes higher, for higher absorption. This behavior is quite well-known from previous studies on azo-polymers, but we present these data here in order to show that light-induced chromophore reorientation is also exhibited by the polymers studied in this work.

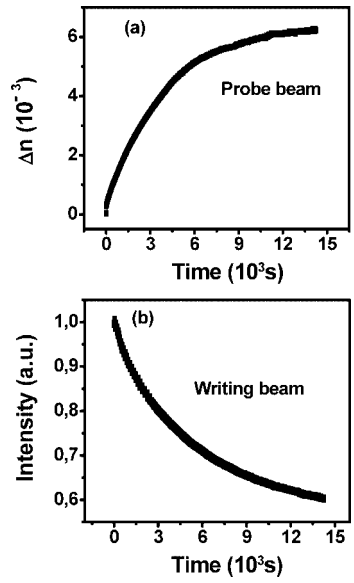

Figure 4. (a) Light-induced birefringence measured as described in the experimental section for a sample of compound **1**. (b) Corresponding decrease in light transmission.

Similar experiments were also carried out without the writing beam, but applying an electric field $E = 20$ V/μm along the normal to the sample, in order to test how well the field can reorient chromophores. However, none of the four compounds showed any field-induced birefringence, as it was expected given their high T_g values.

An interesting behavior was detected by following the intensity of the transmitted writing beam during the birefringence measurements. A typical transmission dependence on illumination time is illustrated in Figure 4b for compound **1**. This behavior was also observed for **2**, but never for **3** and **4**. Considering the trans−cis photoisomerization, the transmission is expected to increase during illumination, as the population of molecular transition dipoles along the

(21) Kumar, G. S.; Neckers, D. C. *Chem. Rev.* **1989**, *89*, 1915.
(22) Todorov, T.; Nikolova, L.; Tomova, N. *Appl. Opt.* **1984**, *23*, 4309.
(23) Delaire, J. A.; Nakatani, K. *Chem. Rev.* **2000**, *100*, 1817.
(24) Natansohn, A.; Rochon, P. *Chem. Rev.* **2002**, *102*, 4139.
(25) Yaroshchuk, O. V.; Dumont, M.; Zakrevskyy, Y. A.; Bidna, T. V.; Lindau, J. *J. Phys. Chem. B* **2004**, *108*, 4647.

polarization of light is depleted. We do not observe such transmission increase, except as an initial trend in very old and oxidized samples (see the Supporting Information, Figure S2). We first considered that the transmission decrease shown in Figure 4b could be attributed to the light scattering due to chromophore aggregation in domains, a phenomenon that often accompanies azo-chromophore light-induced reorientations.[26,27] However, we were not able to detect any increase in scattering due to illumination. Given the fact that **3** and **4**, where strong molecular dipoles are not present, do not exhibit such behavior, one reasonable explanation of the data can be an absorption increase due to the light-induced formation of dipolar aggregates,[28] which modifies absorption due to the shift of the electronic energy levels involved in the transition. These data are presented here for sake of completeness and as further evidence (in addition to light-induced birefringence) of the presence in our materials of light-induced chromophore mobility.

There is another light-induced effect associated with trans−cis isomerization and known to be important in azo-polymers, namely the movement of massive amounts of materials over large distances, even micrometers.[29] This phenomenon, which is important in the well studied, if not completely understood, surface relief gratings formation,[30,31] is active well below T_g. Surface relief gratings (SRGs) can be obtained at room temperature also in the materials under investigation in this article. They have been inscribed on polymer films (thickness ≈ 300 nm) using a Lloyd's mirror arrangement to superimpose left and right circularly polarized interfering beams at $\lambda = 488$ nm (100 mW cm^{-2}) on the sample surface. The surface gratings produced are permanent as long as the temperature of the sample is kept below its T_g. The surface profiles of the film after the creation of the grating were studied by AFM. A typical result is presented in the Supporting Information for **1** (Figure S3). These results show that stable surface structures can be optically written on these azopolymeric substrates with high T_g. The details of such an effect are not important in the context of this work: the relevant issue is that there is experimental evidence pointing at the fact that, well below T_g, light can induce molecular reorientations via conformational rearrangements of the azo-moiety.

Photorefractivity. Two-beam coupling experiments were carried out at room temperature and at $\lambda = 633$ nm, by using the experimental setup schematically illustrated in Figure 5a. The behavior of compound **1**, showing energy exchange between the two writing beams, is also illustrated in Figure 5a. Given the samples thickness $d = 15-40$ μm and the grating period $\Lambda = 3$ μm, the experiments were performed in the Bragg diffraction regime.[32] Therefore, the energy

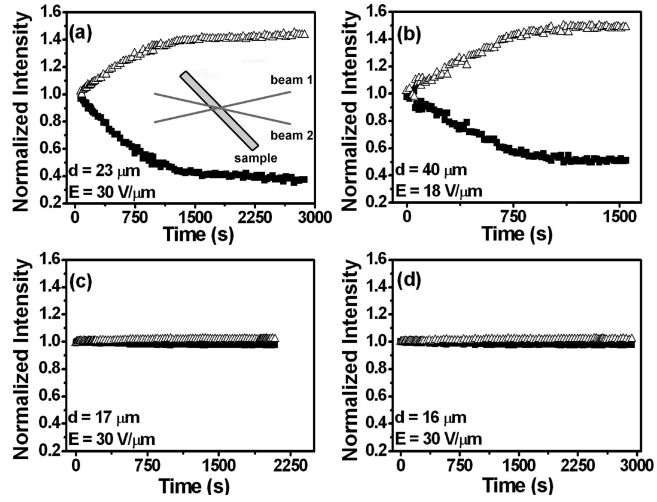

Figure 5. Time evolution of energy exchange between two light beams at $\lambda = 633$ nm during two-beam coupling at room temperature for compounds (a) **1**, (b) **2**, (c) **3**, and (d) **4**. Data for compound **2** have been obtained from a sample containing 20% of the plasticizer DPP. In all cases, the grating period was $\Lambda = 3$ μm, the light intensity was $I = 0.8$ W cm^{-2}. The inset in (a) is a schematic illustration of the experimental setup. All data were rescaled to eliminate the effect of the decreasing total transmission during illumination.

exchange shown in Figure 5a can be taken as a signature of the photorefractive nature of the photoinduced gratings.[5] In addition, the energy exchange reverses when the direction of the applied field is reversed and compound **1** is a photoconductor at $\lambda = 633$ nm (see Table 1). Direct measurements of the phase shift between interference fringes and refractive index were performed by using the moving grating technique.[33] Results, presented in the Supporting Information, not only confirmed the photorefractive nature of the phase grating but also revealed the simultaneous presence of a weaker grating in phase with the light pattern, as expected in azo-compounds where local effects due to the trans−cis isomerization are active.

The fact that photorefractivity is observed more than 120 °C below T_g without prepoling is remarkable. Moreover, the PR performance is considerable: the usual quantitative parameter used to describe PR behavior is the optical gain coefficient Γ, defined as

$$\Gamma = \frac{\cos(\alpha)}{d}\ln\left[\frac{b\gamma}{b+1-\gamma}\right] \qquad (2)$$

where α is the internal angle between the sample normal and the probe beam, $\gamma = I_{probe}(I_{pump} \neq 0)/I_{probe}(I_{pump} = 0)$ is the amplification factor, b is the beam intensity ratio, and d is the sample thickness. For compound **1**, Figure 5a, $\Gamma = 480$ cm^{-1}, a very high value when compared both with absorption ($\alpha = 168$ cm^{-1}) and with literature data.[14] A very similar behavior, even quantitatively, is exhibited by compound **2**, see Figure 5b: this clearly indicates that results do not depend on the fact that the different functionalities reside on the same side-chain, nor they depend on the nature of the chiral spacer. Even if the gain is high, the presence of beam fanning[34] can be excluded, at least for the electric field

(26) Meier, J. G.; Ruhmann, R.; Stumpe, J. *Macromolecules* **2000**, *33*, 843.
(27) Zebger, I.; Rutloh, M.; Hoffmann, U.; Stumpe, J.; Siesler, H. W.; Hvilsted, S. *Macromolecules* **2003**, *36*, 9373.
(28) Eisfeld, A.; Briggs, J. S. *Chem. Phys.* **2006**, *324*, 376.
(29) Cojocariu, C.; Rochon, P. *Pure Appl. Chem.* **2004**, *7−8*, 1479.
(30) Rochon, P.; Batalla, E.; Natansohn, A. *Appl. Phys. Lett.* **1995**, *66*, 136.
(31) Pedersen, T.; Johansen, P.; Holme, N.; Ramanujam, P.; Hvilsted, S. *Phys. Rev. Lett.* **1998**, *80*, 89.
(32) Gaylord, T. K.; Moharam, M. G. *Appl. Opt.* **1981**, *20*, 3271.
(33) Sutter, K.; Günter, P. *J. Opt. Soc. Am., B* **1990**, *7*, 2274.
(34) Grunnet-Jepsen, A.; Thompson, C. L.; Twieg, R. J.; Moerner, W. E. *J. Opt. Soc. Am., B* **1998**, *15*, 901.

intensities that were used, by the fact that the gain just changes sign without showing any other variation when the sign of the applied field is reversed.

The photorefractive properties of amorphous systems based on azo-compounds have been extensively studied. However, this was always done (a) on prepoled high T_g materials[35−38] or (b) above or just below T_g,[39−42] where orientational motions are still active. One work reports photorefractivity in a nonpoled sol−gel glass containing azo moieties,[43] but in these systems the concept of T_g is not meaningful and the amount of residual conformational mobility is an open question. A deeper understanding of the origin of photorefractivity in nonpoled, high T_g polymers, requires an analysis of the different possible light-induced effects on azo-compounds. As shown in the previous section, the materials used in this study exhibit light induced conformational mobility which, in turn, can affect absorption and refractive index. However, these effects are local, in the sense that their extent is proportional to the local light intensity, and therefore they are not expected to contribute to the energy exchange in two-beam coupling. In order to be active within a PR medium, conformational mobility must be coupled to a nonlocal effect, and this is what can happen in photoconducting materials, such as the ones studied in this work. In fact, in this case the nonlocal entity is the photogenerated electric field, which is phase shifted with respect to the light pattern. The field itself would not reorient molecular dipoles so far below T_g, as confirmed by the birefringence measurements, but this is possible in the presence of light-induced conformational mobility.

The observation of energy exchange in the Bragg regime in a photoconducting material already constitutes sufficient experimental evidence in order to claim the role of an electric field in the orientation of chromophores. One further indication can be obtained by comparing the slower time constant of light-induced birefringence with the faster build-up of energy exchange, both measured using the same light intensity. In the case of compound **1**, these data are illustrated in Figures 4a and 5a, respectively. During birefringence measurements no field is applied and birefringence originates from the fact that polarized light absorption (inducing the trans to cis isomerization) is higher for certain molecular orientations, whereas the reverse process (cis to trans) yields random reorientations. In contrast, two-beam coupling is carried out in the presence of an electric field and this could not only make the cis−trans reverse process not random, but it could also induce the reorientation of nonexcited chromophores, by exploiting conformational mobility obtained via the rearrangements of neighboring excited chromophores. Both effects can lead to faster orientation.

The importance of the electric field in the energy exchange experiments we describe may also be inferred by considering the data of panels c and d in Figure 5, obtained at $\lambda = 633$ nm using compounds **3** and **4**, in which the high molecular dipoles associated with the cyano (compound **1**) and nitro (compound **2**) groups are not present. As a consequence, field-induced molecular reorientation is much less effective and energy exchange is greatly reduced, with a gain coefficient $\Gamma \approx 30\ cm^{-1}$. The same values of Γ were obtained for **3** and **4** in measurements at $\lambda = 532$ nm, where their absorption is higher, ruling out the possibility that their lower PR performance at $\lambda = 633$ nm is a consequence of their lower absorption (see Table 1). It should be underlined that, given a certain degree of field-induced orientation, the contribution of permanent dipoles to birefringence is expected to be negligible because the dipolar reorientation contribution to polarizability is not active at optical frequencies. In other words, the main contribution of permanent dipole moments to the refractive index modulation is expected to be only indirect, through the reorienting effect of the DC space-charge field. This was confirmed by birefringence measurements on mechanically oriented samples of **2** (with a polar chromophore) and **3** (with a nonpolar chromophore), which gave similar values of birefringence for the two compounds. These measurements are described in the Supporting Information.

All the experimental evidence illustrated above shows that, in our materials, conformational motions due to isomerization cannot account for PR behavior if the coupling with a field is not present. In addition, given the similar optical gain measured for **3** and **4**, and comparing with the results obtained for **1** and **2**, it is possible to conclude that both absorption and photoconductivity variations (see Table 1) play a secondary role in determining the gain. An extensive and detailed investigation of the optical gain obtained with no applied field in a nonphotoconducting system based on an azo-dye was recently published.[44] The observed gain was linked to the photoisomerization process using a phenomenological model, showing that energy exchange in azo-compounds is a process not yet fully understood, regardless of their photoconductivity. Our data show that, at least in the materials we investigated, PR performance cannot be linked to the simple photoisomerization. The whole picture is instead consistent with a field-induced, light-assisted (via the isomerization) chromophore reorientation mechanism for the PR behavior in high T_g azo-polymers.

Influence of Light Absorption. With the aim of increasing the speed of the effect, we performed two-beam coupling experiments on compound **1** at $\lambda = 532$ nm, where the absorption coefficient $\alpha = 1810\ cm^{-1}$ is much higher than at $\lambda = 633$ nm. The same light intensity was used at the two wavelengths. Results, as illustrated in Figure 6, show that at $\lambda = 532$ nm the time constant of the build-up of the refractive index modulation is τ ($\lambda = 532$ nm) ≈ 5 s, 2 orders of

(35) Hattemer, E.; Zentel, R.; Mecher, E.; Meerholz, K. *Macromolecules* **2000**, *33*, 1972.
(36) Chen, Y. W.; He, Y. K.; Chen, H. Y.; Wang, F.; Chen, Z. J.; Gong, Q. H. *J. Appl. Polym. Sci.* **2000**, *77*, 189.
(37) Iftime, G.; Lagugnè Labarthet, F.; Natansohn, A.; Rochon, P.; Murti, K. *Chem. Mater.* **2002**, *14*, 168.
(38) Hua, J.; Li, Z.; Qin, J.; Li, S.; Ye, C.; Lu, Z. *React. Funct. Polym.* **2007**, *67*, 25.
(39) Hwang, J.; Sohn, J.; Park, S. Y. *Macromolecules* **2003**, *36*, 7970.
(40) Kou, H.; Shi, W. *Eur. Polym. J.* **2004**, *40*, 1337.
(41) Shi, J.; Huang, M.; Chen, Z.; Gong, Q.; Cao, S. *J. Mater. Sci.* **2004**, *39*, 3783.
(42) Zhang, L.; Huang, M.; Jiang, Z.; Yang, Z.; Chen, Z.; Gong, Q.; Cao, S. *React. Funct. Polym* **2006**, *66*, 1404.
(43) Cheben, P.; del Monte, F.; Worsfold, D. J.; Carlsson, D. J.; Grover, C. P.; Mackenzie, J. D. *Nature* **2000**, *408*, 64.
(44) Gallego-Gòmez, F.; Del Monte, F.; Meerholz, K. *Nat. Mater.* **2008**, *7*, 490.

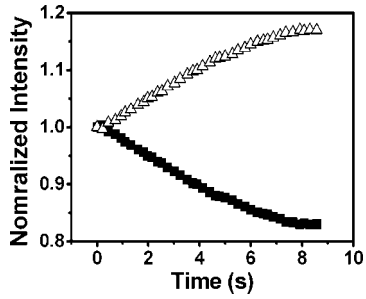

Figure 6. Time evolution of energy exchange at $\lambda = 532$ nm during two-beam coupling at room temperature for compound **1**. The sample thickness was $d = 32$ μm, the grating period was $\Lambda = 3$ μm, the applied field was $E = 22$ V/ μm, and the light intensity was $I = 0.8$ W cm^{-2}.

magnitude smaller than at $\lambda = 633$ nm. As the photoconductivity in our compounds is even higher than the photoconductivity exhibited by other PR polymers with faster response, it seems reasonable that the rate limiting factor for the PR grating build-up is not the setup of the photogenerated electric field, but the reorientation of chromophores. The result illustrated in Figure 6 then highlights the role played by the rate of photo-orientation in determining the overall writing time of the hologram.

In addition, the same experiments carried out at $\lambda = 532$ nm on **3** and **4** (both with nonpolar chromophores), show a decrease in the time constant of the grating build-up by only a factor 2 when compared to the time constant of the grating build-up at $\lambda = 633$ nm. The different behavior exhibited in this respect by different polymers, depending on the polarity of the chromophore, underlines again the importance of the dipole/field interaction in the photo-orientation, and ultimately in the PR performance, of nonpoled, high T_g organic materials.

Conclusion

In this work, we showed how the photorefractive properties of nonpoled azo-polymers can be observed at more than 100 °C below their glass transition temperature. Although light-activated conformational mobility is a necessary requirement at such temperatures, an electric field (applied + photogenerated) is also necessary in order to encode a phase-shifted hologram, via the reorientation of polar chromophores. Our data indicate that the conformational mobility of interest when considering macroscopic photorefractive index modulations is not the simple trans−cis isomerization by itself, but a chromophore reorientation process induced by the electric field and assisted by the photoisomerization. In polymers with polar chromophores, the writing time of the refractive index modulation, which is long at lower absorption, was found to decrease by 2 orders of magnitude upon using illumination at a wavelength where absorption is higher.

Acknowledgment. The authors thank Dr. A. Pane for providing the conducting substrates used for the measurements. The authors also thank Prof. Danilo Pedron and Dr. Tiziano Dainese for the SRG inscriptions and relative AFM measurements on amorphous polymeric thin films and Prof. C. Versace for the birefringence measurements at the optical microscope. This work has been supported by MiUR through the Centro di Eccellenza CEMIF.CAL (CLAB01TYEF) and the PRIN 2007 (2007WJMF2W) projects.

Supporting Information Available: Chemical synthesis and characterization, TGA results, light transmission, optically induced surface relief gratings, measurements of grating/interference phase shift, birefringence in mechanically oriented samples (PDF). This information is available free of charge via the Internet at http://pubs.acs.org.

CM8034664